PHYSICAL REVIEW B VOLUME 32, NUMBER 6 15 SEPTEMBER 1985

Quasiparticle band structure of lithium hydride

S. Baroni*
Institut de Physique Théorique Ecole Polytechnique Fédérale de Lausanne, CH-1015 Lausanne, Switzerland

G. Pastori Parravicini and G. Pezzica
Dipartimento di Fisica, Università di Pisa and Gruppo Nazionale di Struttura della Materia del Consiglio Nazionale delle Ricerche, Piazza Torricelli 2, 56100 Pisa, Italy
(Received 27 February 1985)

We consider the energy bands of quasielectrons and quasiholes in lithium hydride within the Coulomb-hole—plus—screened-exchange formalism. The crystal density matrix is expressed by means of localized Gaussian functions and off-diagonal terms are preserved and rigorously accounted for. Using a basis set of plane waves orthogonalized to the cation core wave function, we express the matrix elements of the nonlocal self-energy operator in analytic form, thus achieving high numerical accuracy with moderate computational labor. Our theoretical results for the quasiparticle band structure, the valence bandwidth, the energy gap, and exciton resonances are in good agreement with the available optical and photoemission data. *Ab initio* inclusion of the many-body effects is found to be a key point for a theoretical interpretation of experimental electron properties and transitions in LiH.

I. INTRODUCTION

A sound theoretical description of the electronic structure of solids cannot be achieved without handling directly the equations of motion obeyed by the one-particle Green's function of the many-electron system. The independent-particle approximations, on which considerable efforts have been focused in the literature,[1] constitute an important but only a preliminary step toward a quantitative account of the electronic excitations in the solids.

The many-body theory of quasiparticles (QP's) in solids has been systematically developed and reviewed in the literature;[2,3] the simplest many-body approach which includes *ab initio* correlation polarization effects in the concept of energy bands is known as the Coulomb-hole—plus—screened-exchange approximation[2] (COHSEX). Soon after the appearance of this basic theoretical framework, it was applied to semiconductors[4] and to insulators.[5] However, in the papers mentioned,[4,5] the numerical evaluation of the exchange and correlation effects was so laborious as to discourage for a decade or so further studies of energy bands based on the Coulomb-hole—and—dynamically-screened-exchange approximation (except for the perturbative version of Brener[6]).

Another source of the delay operating against systematic application of the many-body formalism can probably be ascribed to the concomitant developments of the density-functional formalism.[7] Within this formalism, the treatment of exchange and correlation with various approximations has heuristically succeeded in describing a number of ground-state properties of solids. However, the situation is less satisfactory for interpreting single-particle excitations; furthermore, from a first-principles point of view it is not clear what kinds of many-body effects are actually included in the local-density formalism.

More recently a renewed interest has focused on the fundamentals of first-principles calculations within the Green's-function method. The formalism has been revised to obtain physically and mathematically sound approaches to the complicated self-energy operator.[8] Furthermore, efficient techniques[9] have become available to treat rigorously the integro-differential equations which describe the elementary excitations in solids; using appropriately localized Gaussian-type orbitals[10] (GTO's) and orthogonalized plane waves[11] (OPW's), the matrix elements of the nonlocal self-energy operator can be calculated by analytical means in the COHSEX approximation.

In this paper we consider specifically the quasiparticle states in solid lithium hydride, which constitutes the simplest heteronuclear crystal. The quantum-mechanical investigation of its structure has been pursued from the pioneering work of Hylleraas[12] up to the recent Hartree-Fock (HF) work of Dovesi *et al.*[13] In spite of its simplicity and of the numerous theoretical and experimental investigations, a quantitative understanding of the electronic excitations of this pilot compound is still lacking. In this paper for the first time we calculate *ab initio* the quasiparticle band structure of LiH and show that a proper account of the many-body effects is central to bring into agreement theoretical and experimental results.

Calculations on the energy bands of LiH have been carried out by several authors with different methods. The first calculation was performed by Ewing and Seitz,[14] who used the cellular method. An important contribution was that of Kunz and Mickish,[15] who also treated correlation polarization effects within the electronic polaron model.

Ermoshkin and Evarestov[16] used a cluster model for the perfect crystal and for a number of embedded point defects. Perrot[17] applied an appropriate version of the augmented-plane-wave (APW) method. Kulikov[18] exploited a linearized Korringa-Kohn-Rostoker method in the version implemented by Ziman (KKRZ). Grosso and Pastori Parravicini[19] performed a Hartree-Fock calculation within the orthogonalized-plane-wave method; they introduced a Gaussian representation of atomiclike orbitals and assumed an *ad hoc* diagonal density matrix. Finally, Dovesi *et al.*[13] performed a HF study using a polarizable basis set of localized orbitals.

Despite these extensive efforts,[13–19] substantial quantitative disagreement occurs among the various calculations even for the interpretation of basic experimental properties, such as the valence bandwidth and the forbidden gap. This appears even more surprising if one considers that LiH, which crystallizes in the highly symmetric fcc structure, is the simplest of all binary compounds. In fact, in the generally adopted ionic picture, all four electrons in the unit cell have s-like character and only two of them are really relevant for the chemical bonding.

In this paper we show that the discrepancy between theory and experiment is substantially removed if a many-body approach is adopted for describing the quasiparticle band structure of LiH. Particular attention has been given to a correct account of orthogonalization effects; due to the diffuse nature of the hydride-ion wave function, a large number of neighbors must be taken into consideration. Even in this peculiar situation, we succeed in expressing the matrix elements of the nonlocal self-energy operator in analytic form; this technical part is discussed in the Appendix. In Sec. II we briefly summarize the basic equations encountered in the Coulomb-hole—and—dynamically-screened-exchange approximation. The density matrix for LiH crystals and a suitable model dielectric function are also provided. In Sec. III we report the results of our calculations and compare them with the theoretical and experimental data available in the literature. Section IV contains the conclusions.

II. SUMMARY OF THE FORMALISM

A. Discussion of the quasiparticle equations

The calculations of the present paper are based on the Coulomb-hole—plus—screened-exchange approximation proposed by Hedin[2] and extended by Hedin and Lundqvist.[3] In essence, this formalism considers the dynamics of the one-particle Green's function and then expands the self-energy operator in terms of a dynamically screened interaction (rather than a bare Coulomb interaction), keeping the first term. The quasiparticle excitations in a closed-shell many-electron system (such as LiH) obey the integro-differential equation

$$\left[\frac{\mathbf{p}^2}{2m}+V_N(\mathbf{r})+V(\mathbf{r})\right]\psi(\mathbf{r}) + \int \Sigma(\mathbf{r},\mathbf{r}',E)\psi(\mathbf{r}')d\mathbf{r}'=E\psi(\mathbf{r}) , \quad (1)$$

where V_N is the nuclear Coulomb potential, $V(\mathbf{r})$ is the Hartree potential of the electrons, and Σ is the self-energy operator which includes all the exchange and correlation effects. In terms of the spin-independent one-electron density matrix $\rho(\mathbf{r},\mathbf{r}')$ we can write

$$V(\mathbf{r})=\int \frac{e^2}{|\mathbf{r}-\mathbf{r}'|}\rho(\mathbf{r}',\mathbf{r}')d\mathbf{r}' . \quad (2)$$

In general, the difficulty in solving Eq. (1) is related to the fact that $\Sigma(\mathbf{r},\mathbf{r}',E)$ is a complicated, nonlocal energy-dependent operator.

In the Hartree-Fock approximation the self-energy operator is replaced by

$$\Sigma_{\mathrm{HF}}(\mathbf{r},\mathbf{r}')=-\tfrac{1}{2}\rho(\mathbf{r},\mathbf{r}')\frac{e^2}{|\mathbf{r}-\mathbf{r}'|} . \quad (3)$$

The previous theoretical works on LiH were concerned, at least in principle, with the solution of Eq. (1) with the kernel as in Eq. (3).

As already discussed, the COHSEX approximation constitutes one of the biggest steps in the theoretical basis for band calculations. In the COHSEX formalism the self-energy operator is approximated[3] by

$$\Sigma_{\mathrm{COHSEX}}(\mathbf{r},\mathbf{r}')=-\tfrac{1}{2}\rho(\mathbf{r},\mathbf{r}')W(\mathbf{r}-\mathbf{r}')+E_{\mathrm{CH}}\delta(\mathbf{r}-\mathbf{r}') , \quad (4)$$

where $W(\mathbf{r}-\mathbf{r}')$ is the statically screened Coulomb interaction and the Coulomb hole energy is given by

$$E_{\mathrm{CH}}=\tfrac{1}{2}\int \frac{1}{(2\pi)^3}d\mathbf{q}\frac{4\pi e^2}{q^2}\left[\frac{1}{\epsilon(\mathbf{q})}-1\right] . \quad (5)$$

In Eq. (4) it is assumed that the dielectric screening is homogeneous and local field effects can be neglected.[3,9] The quasiparticle band structure of LiH provided in the present paper is obtained solving the integro-differential equation (1) with the kernel (4). Some relevant details concerning two ingredients that we need, namely, the density matrix and the dielectric screening in LiH crystals, are briefly discussed below.

B. Density matrix for LiH crystals

The crystal structure of LiH is fcc with two ions in the unit cell, H^- in the position $\mathbf{d}_1=\mathbf{0}$ and Li^+ in the position $\mathbf{d}_2=(a/2)(1,0,0)$. The lattice constant[20] a is taken to be $a=7.720$ a.u. In the ionic picture, cations and anions have the simple $1s^2$ closed-shell configuration. The localized wave functions, following the work of Hurst,[21] were recalculated for our purpose and expanded in Gaussian orbitals.[22]

The computation of the electron band structure requires the knowledge of the first-order density matrix[23] of the electron system. In the minimal basis set for the closed-shell LiH system, the spinless density matrix can be written as

$$\rho(\mathbf{r},\mathbf{r})=2\sum_{\alpha,\beta}\sum_{\tau_m,\tau_n}\phi_\alpha^*(\mathbf{r}-\mathbf{d}_\alpha-\tau_m)(S^{-1})_{\alpha m,\beta n} \times\phi_\beta(\mathbf{r}'-\mathbf{d}_\beta-\tau_n) , \quad (6)$$

where τ_m,τ_n are translational vectors, α,β label either hydride or lithium ions, and S is the overlap matrix

$$S_{\alpha m,\beta n}=\langle\phi_\alpha(\mathbf{r}-\mathbf{d}_\alpha-\tau_m)\,|\,\phi_\beta(\mathbf{r}-\mathbf{d}_\beta-\tau_n)\rangle\ . \tag{7}$$

Because of the diffuse nature of the hydride-ion wave function, the inversion of the overlap matrix must be performed nonperturbatively and include a sufficient number of shells. This peculiar aspect of orthogonalization effects was first pointed out by Berggren and Martino[24] and has been extensively studied in the literature.[25] As we shall see, a proper account of orthogonalization effects is essential also in connection with band-structure calculations.

C. Dielectric screening for LiH

In the literature there are a number of model dielectric functions, which allow a satisfactory description of screening effects in semiconductors and insulators.[26] In this paper we find it convenient to adopt the interpolation formula[9]

$$\frac{1}{\epsilon(q)}=\frac{1}{\epsilon_0}+c_1\frac{q^2}{q^2+k_1^2}+c_2\frac{q^2}{q^2+k_2^2}\ . \tag{8}$$

The advantages of this interpolation formula are the following.

(i) Each term in Eq. (8) gives rise to an effective interaction in real space of the Yukawa type, and the corresponding matrix elements can be evaluated in closed analytic form (see the Appendix).

(ii) We can determine the parameters in Eq. (8) in such a way as to reproduce the expected behavior of $\epsilon(q)$ for low-, intermediate-, and high-q limits. We will comment more explicitly on this point.

The correct low-q limit in Eq. (8) is obtained by setting ϵ_0 equal to the electronic contribution to the static dielectric constant; from Ref. 27 we set $\epsilon_0=3.61$. We also require that the value of one of the screening parameters, say, k_1 is the same as that provided from a Thomas-Fermi treatment.[28]

In order to fix the remaining three parameters, we notice that for high q the behavior of $\epsilon(q)$ must be of the form

$$\frac{1}{\epsilon(q)}\to 1-\frac{16\pi n_e}{a_B}\frac{1}{q^4}+O\left[\frac{1}{q^6}\right]\quad\text{as } q\to\infty\ , \tag{9}$$

where n_e is the valence-electron density and a_B is the Bohr radius. In the asymptotic behavior (9), the term of type q^{-2} must be rigorously lacking, as can be inferred also from the fact that its presence would give rise to unphysical divergences in the response to a point-charge perturbation.

The above criteria completely determine the parameters in Eq. (8); we have verified that other reasonable choices based on models (see Ref. 26) lead to similar results and do not influence appreciably the final calculations. The actual values of the parameters used in Eq. (8) are $c_1=1.144$, $k_1=0.817$, $c_2=-0.421$, $k_2=1.346$; the value of the Coulomb-hole energy, defined by Eq. (5), is $E_{\mathrm{CH}}=-5.01$ eV.

III. RESULTS OF CALCULATIONS

A. General remarks

Within the formalism outlined in the preceding section, it is now very economical to calculate the band structure of LiH in the HF approximation and the quasiparticle band structure in the COHSEX approximation. We have performed both types of calculations in order to single out and discuss the role of the many-body effects. As an expansion set we have used plane waves orthogonalized to the cation core wave function.

The energy of the core states in the crystal has been determined with the following procedure. In the case of HF calculations, the theoretical orbital energy for the free Li^+ ion with seven optimized Gaussians is found to be $\epsilon=-75.97$ eV, which differs by less than 0.35 eV from the experimental ionization limit[29] ($I_p=75.6193\pm0.0031$ eV). The position of the HF core band can be obtained[30] from the relation $E_{\mathrm{core}}^{\mathrm{HF}}=\epsilon+\alpha_m e^2/a+\delta$, where $\alpha_m=3.495\,13$ is the Madelung constant, $\alpha_m e^2/a=12.31$ eV is the potential of the surrounding lattice of point ions, and $\delta=-0.44$ eV is the correction due to the finite size of the hydride ions in the first few shells. For the core energy in the HF calculations, we thus have $E_{\mathrm{core}}^{\mathrm{HF}}=-64.10$ eV. The position of the COHSEX core band is modified because of the screening of the ionic self-energy operator with the crystal dielectric function. This shift can be safely obtained with a perturbative approach[6] because of the small spatial extent of the cation core wave function. We obtain $E_{\mathrm{core}}^{\mathrm{COHSEX}}=-59.94$ eV, the difference with respect to the corresponding HF value being, of course, of the same order as the Coulomb-hole term. Now we will pass on to present calculations and discuss our results.

B. Hartree-Fock energy bands

In Fig. 1 we report our results for the HF energy bands of LiH; the crystal energies at some symmetry point of interest are given in Table I. The states are labeled with the irreducible representations of the little groups of $\mathbf{k}$, following the notations of Koster *et al.*[31] A few additional details on our calculations are worthwhile to mention.

The cutoff in kinetic energy of the plane waves has been chosen as $16(2\pi/a)^2$ Ry because this assures a satisfactory accuracy; this corresponds to including a number of OPW's between 60 or 70 (depending on the point $\mathbf{k}$ of interest). Occasionally, we have performed test calculations with as many as two hundred OPW's. In the inversion of the overlap matrix (which is the most peculiar aspect of LiH), we have included up to seven shells; this corresponds to considering the interaction between the central ion with the first 80 neighbor atoms. The diffuse nature of the hydride-ion wave functions makes this compound a nontrivial challenge for band-structure methods.

We wish to insist on this particular aspect with a few more considerations. In Fig. 2 we show the behavior of the valence energy band (described here with a single OPW in order to keep to the essential) when increasing the number of interacting shells. The relative maximum of $E_v(\mathbf{k})$ for small $\mathbf{k}$ exhibited by some curve in Fig. 2 is totally due to the fact that only a small number of neigh-

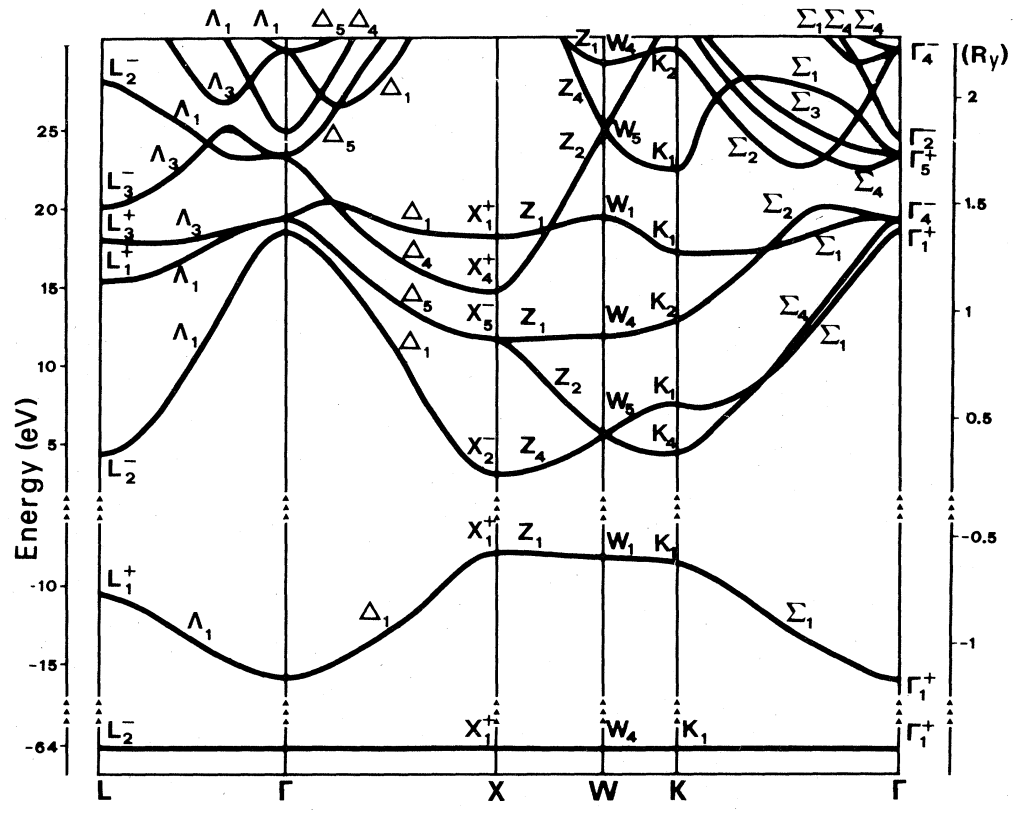

FIG. 1. Hartree-Fock band structure of solid lithium hydride.

bor ions were considered. This spurious behavior disappears when a proper number of shells is included. A spurious effect of similar origin, concerning the isotropic Compton profile, was earlier noticed by Paakkari *et al.*[32]

In order to evaluate quantitatively the effects of off-diagonal terms in the density matrix we have performed HF calculations, replacing in Eq. (6), $(S^{-1})_{\alpha m,\beta n}$ by $\delta_{\alpha\beta,mn}$. The results are reported in Fig. 3; the central importance of a proper account of orthogonalization effects for a correct description of the valence band is evident. The results of Fig. 3 on one hand justify qualitatively the "*ad hoc*" procedure, adopted in Ref. 19, which consisted of simulating the orthogonalization effect by a suitable narrowing of the hydride-ion wave function; on the other hand, the results of Fig. 3 show that a quantitative analysis of the band structure of LiH can only be pursued with an accurate description of the density matrix of the crystal.

The features mentioned above are the primary source of the differences, at times remarkable, occurring among the

TABLE I. Energies in eV of Hartree-Fock calculations in LiH at high symmetry points of the Brillouin zone: Γ ($\mathbf{k}=\mathbf{0}$), X [$\mathbf{k}=(2\pi/a)(1,0,0)$], L [$\mathbf{k}=(2\pi/a)(\frac{1}{2},\frac{1}{2},\frac{1}{2})$], K [$\mathbf{k}=(2\pi/a)(\frac{3}{4},\frac{3}{4},0)$], and W [$\mathbf{k}=(2\pi/a)(1,\frac{1}{2},0)$].

Core states	Γ_1^+	−64.10	X_1^+	−64.10	L_2^-	−64.10	K_1	−64.10	W_4	−64.10
Valence states	Γ_1^+	−15.97	X_1^+	−7.77	L_1^+	−10.60	K_1	−8.32	W_1	−8.09
Conduction states	Γ_1^+	18.72	X_2^-	3.03	L_2^-	4.42	K_4	4.36	W_5	5.64
	Γ_4^-	19.53	X_5^-	11.77	L_1^+	15.41	K_1	7.80	W_4	12.01
	Γ_5^+	23.45	X_4^+	14.71	L_3^+	18.00	K_2	12.98	W_1	19.67
	Γ_2^-	24.64	X_1^+	18.27	L_3^-	20.10	K_1	17.18	W_5	25.14

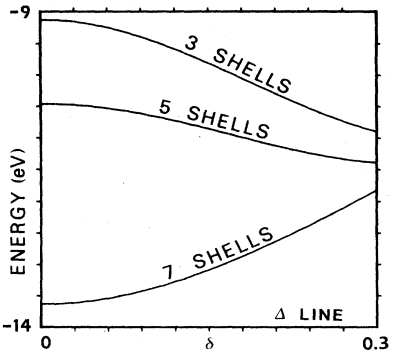

FIG. 2. Behavior of the valence band along the line Δ [$\mathbf{k}=(2\pi/a)(\delta,0,0)$] using a single OPW. The number of shells exploited for inverting the overlap matrix is indicated.

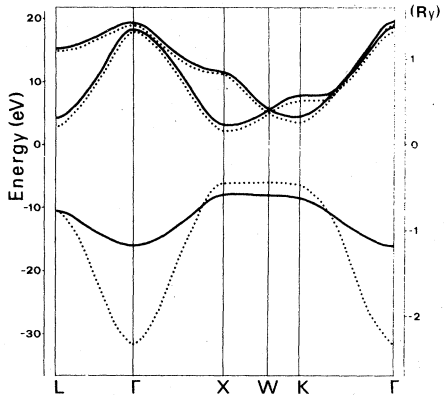

FIG. 3. Comparison between the HF band structure obtained with the rigorous density matrix (solid curve) and the HF band structure with the density matrix in diagonal form (dotted curve).

theoretical calculations available in the literature. In Table II we report some relevant energies as calculated by different authors, together with the rigorous HF calculations of the present work.

The sequence of levels of the valence and conduction bands in LiH can be qualitatively understood starting from the "empty-lattice" analysis of the NaCl structure[33] and considering the interaction between states of the same symmetry by perturbation theory.[34] For convenience, in Fig. 4 we show the empty-lattice band structure. To understand qualitatively the relationship between Figs. 1 and 4, we notice that at each $\mathbf{k}$ vector the lowest s-like empty-lattice state splits off in the actual LiH crystal in order to give the corresponding s-like valence band. The remaining accidental degeneracies of the empty lattice are then removed in agreement with the qualitative rules of the perturbation theory. For instance, at point Γ we have in the empty lattice the sequence

$$\Gamma_1^+ \ll \Gamma_1^+,\Gamma_4^-,\Gamma_5^+,\Gamma_2^- < \Gamma_1^+,\Gamma_3^+,\Gamma_4^-,\ldots .$$

The lowest Γ_1^+ state corresponds to the bottom of the valence band. The degeneracy among the states

TABLE II. Energies (in eV) of LiH at some symmetry points determined by different authors and different methods in the one-electron approximation. LCAO denotes the method of linear combination of atomic orbitals.

	Present work, OPW	Dovesi *et al.*, LCAO[a]	Kulikov, KKRZ[b]	Perrot, APW[c]	Kunz and Mickish, LCAO[d]	Ermoshkin and Evarestov, cluster method[e]	Ewing and Seitz, cellular method[f]
X_{1v}^+	−7.77	−6.73	3.3	4.5	−5.4	−13.0	
X_{2c}^-	3.03	6.61	7.0	6.8	8.4		
$E_G=X_{1v}^+\rightarrow X_{2c}^-$	10.80	13.33	3.7	2.3	13.8	12.6	6.8
Γ_{1v}^+	−15.97	−13.39	−1.2	−1.4	−19.3	−15.8	
Γ_{4c}^-	19.53			21.3	21.2		
$\Gamma_{1v}^+\rightarrow\Gamma_{4c}^-$	35.50			22.7	40.5		17.9
$\Delta_v=X_{1v}^+\rightarrow\Gamma_{1v}^+$	8.20	6.67	4.5	5.6	13.7	2.8	3.0
L_{1v}^+	−10.60	−10.57	1.2	2.3	−9.2		
L_{2c}^-	4.42		8.9	9.1	10.4		
$L_{1v}^+\rightarrow L_{2c}^-$	15.02		7.7	6.8	19.6		
$X_{1,\text{core}}^+\rightarrow X_{2c}^-$	67.13	70.35			73.7		

[a] Reference 13.
[b] Reference 18.
[c] Reference 17.
[d] Reference 15.
[e] Reference 16.
[f] Reference 14.

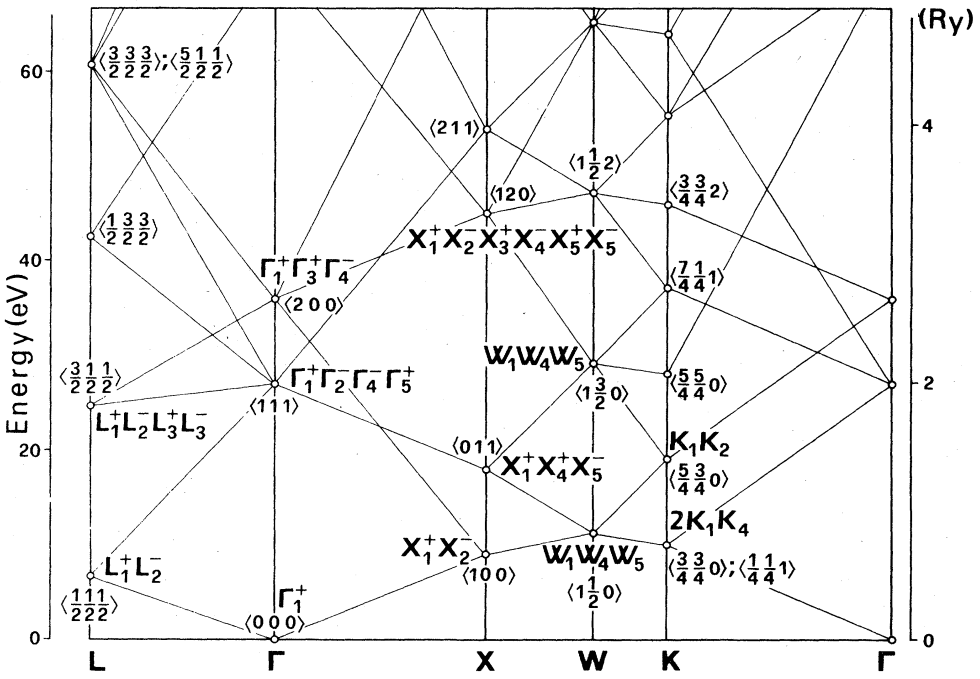

FIG. 4. Empty-lattice energy bands for face-centered-cubic lattices.

$\Gamma_1^+,\Gamma_4^-,\Gamma_5^+,\Gamma_2^-$, corresponding to the plane waves $(2\pi/a)(1,1,1)$, is lifted taking into account the interaction with the states of the same symmetry on different shells of wave vectors; the interaction with the plane waves of type $(2\pi/a)(2,0,0)$ tends to decrease Γ_1^+,Γ_4^- with respect to Γ_5^+,Γ_2^-, and the sequence of conduction states is in fact $\Gamma_1^+ < \Gamma_4^- < \Gamma_5^+ < \Gamma_2^-$.

Similarly at point X we have the empty-lattice sequence

$$X_1^+,X_2^- < X_1^+,X_4^+,X_5^- \ll X_1^+,X_2^-,X_3^+,X_4^-,X_5^+,X_5^- \ldots .$$

We thus expect that the valence band has symmetry X_1^+, and that the lowest conduction states have the sequence $X_2^- < X_5^- < X_4^+ < X_1^+$, as confirmed by Fig. 1.

A similar analysis can be applied to the other symmetry points. According to these qualitative remarks confirmed by the detailed calculations, we see that the valence band and the lowest part of the conduction band are s- and p-like, respectively. This situation is reversed with respect to standard alkali halides.[33–35] Since p bands (s bands) bend downward (upward) as the wave vector $\mathbf{k}$ changes from the center of the Brillouin zone toward the borders, we immediately understand why the direct gap of this material occurs at the point X of the Brillouin zone and not as its center. Another consequent feature is the strong anisotropy of the effective masses of the holes in the valence band at X; notice in fact the strong dispersion along the X-Γ direction against the almost negligible dispersion in the direction X-W perpendicular to it. We finally note that the band structure of solid hydrogen exhibits similar aspects, whose origin is ultimately related to the s nature of the occupied molecular orbital.[36,37]

While the qualitative features of the HF bands are well established (and valid also for correlated energy bands) the quantitative agreement of rigorous HF results with experimental data is poor. For instance, the HF energy gap in our calculation is 10.80 eV, while the experimental gap is $\simeq$5 eV. The HF valence bandwidth is 8.20 eV against experimental values of $\simeq$6 eV. Also the core-conduction edge, estimated experimentally as $\simeq$59–60 eV, is in the HF calculations equal to 67.10 eV. These discrepancies can be removed only by handling from the very beginning the dynamical equations of the one-particle Green's function.

C. Quasiparticle energy bands and comparison with experimental data

Using the formalism outlined in Sec. II, we have calculated the quasiparticle energy bands of LiH within the Coulomb-hole–pulse–screened-exchange approximation. In Fig. 5 we report the QP energy bands. The calculated energies at some symmetry points of interest are given in Table III: for convenience, also the effective masses of quasiparticles are computed and reported in Table IV.

From a comparison between Figs. 1 and 5, we see that, as expected, the core and valence QP energy bands shift upward and the QP conduction bands shift downward; however, these shifts are not "rigid" as in rare-gas solids or alkali halides. This in turn is related to the complicated nature of the valence band, whose width is narrowed by many-body effects. Another important modification is the change of the energy gap; the QP energy gap is 5.24

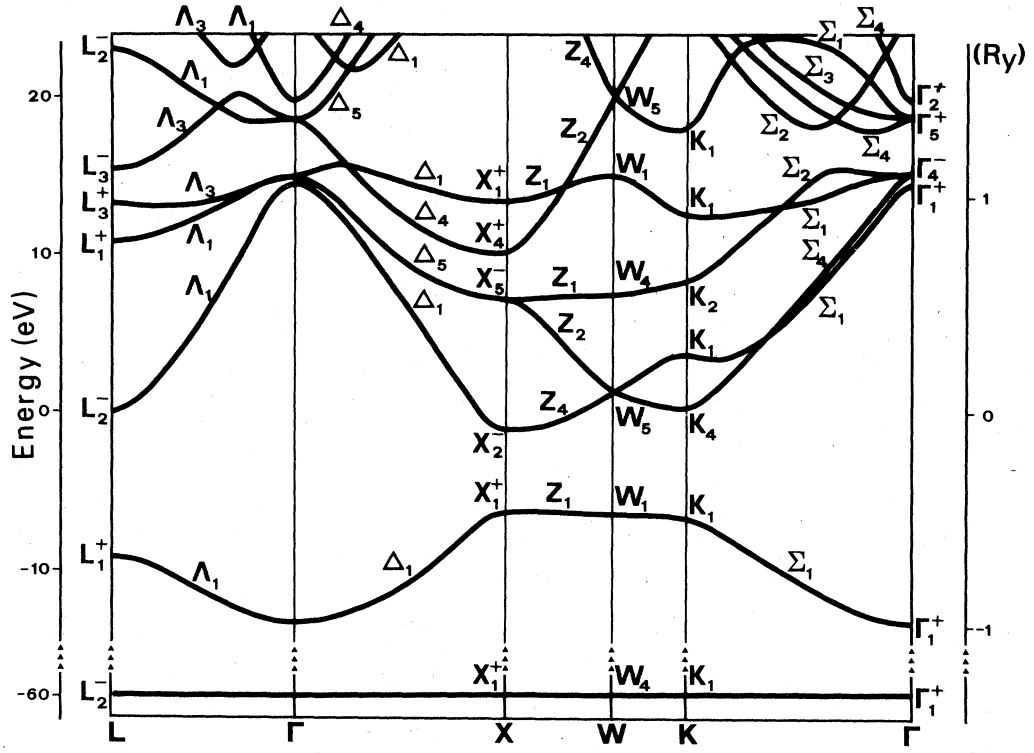

FIG. 5. Quasiparticle band structure of solid lithium hydride.

eV, in comparison with the HF energy gap of 10.80 eV and with the experimental energy gap of 4.99 eV. Also, the energy threshold for core excitons changes drastically, again with a considerable improvement in the agreement with experimental data.

The electronic structure of LiH has been widely investigated experimentally[38–45] by means of reflectivity measurements at the fundamental edge, x-ray photoelectron spectroscopy, synchrotron radiation, and soft-x-ray photoelectric yield spectroscopy. In Table V we compare our theoretical results with experimental data of relevance.

The optical measurements at the fundamental edge are quite accurate and in substantial agreement among themselves.[38–44] The transition $X_{1v}^{+} \rightarrow X_{2c}^{-}$ is dipole allowed and the experimentalists have observed clearly the $n=1$ exciton, the series partner $n=2$, and the one-phonon sidebands. The fine structure of the phonon sidebands, as well as the optical phonon replica, is favored by the high anisotropy of the exciton bands (as can be seen from Table IV). In the effective-mass approximation for shallow excitons, we expect that the effective dielectric constant is close to the static value[27] $\epsilon_s = 12.9 \pm 0.5$. Using the QP masses of Table IV, we obtain for the binding energy of the valence exciton the theoretical value $E_b = +44$ meV, in excellent agreement with the experimental data.

Besides the prominent peaks related to the valence-exciton resonances, other weaker structures were observed in the interband transitions to higher conduction states

TABLE III. Energies (in eV) of the COHSEX calculations in LiH at high symmetry points of the Brillouin zone.

Core states	Γ_1^+	−59.94	X_1^+	−59.94	L_2^-	−59.94	K_1	−59.94	W_4	−59.94
Valence states	Γ_1^+	−13.52	X_1^+	−6.36	L_1^+	−9.23	K_1	−6.86	W_1	−6.56
Conduction states	Γ_1^+	14.21	X_2^-	−1.12	L_2^-	0.22	K_4	0.11	W_5	1.30
	Γ_4^-	14.79	X_5^-	7.22	L_1^+	10.93	K_1	3.41	W_4	7.37
	Γ_5^-	18.57	X_4^+	9.91	L_3^+	13.17	K_2	8.38	W_1	14.94
	Γ_2^-	19.71	X_1^+	13.37	L_3^-	15.45	K_1	12.35	W_5	20.23

TABLE IV. Longitudinal, transverse, and weighted-averaged effective masses (in units of the free-electron mass) for quasiparticles at high symmetry points of the Brillouin zone. The reduced masses for some relevant direct transitions are also given.

Γ_{1v}	$m_l=m_t=0.748$		
Γ_{1c}^{+}	$m_l=m_t=-0.018$		
X_{1v}^{+}	$m_l=-0.150$	$m_t=-4.304$	$\langle m\rangle=-2.919$
X_{2c}^{-}	$m_l=0.121$	$m_t=0.938$	$\langle m\rangle=0.666$
L_{1v}^{+}	$m_l=-0.171$	$m_t=-0.610$	$\langle m\rangle=-0.464$
L_{2c}^{-}	$m_l=0.137$	$m_t=0.142$	$\langle m\rangle=0.140$
$X_{1v}^{+}\rightarrow X_{2c}^{-}$	$\mu_l=0.067$	$\mu_t=0.770$	$\langle\mu\rangle=0.542$
$L_{1v}^{+}\rightarrow L_{2c}^{-}$	$\mu_l=0.076$	$\mu_t=0.115$	$\langle\mu\rangle=0.108$

above $\simeq$5 and $\simeq$10 eV in the absorption spectrum.[44] According to our results of Table III, these structures could be related to the dipole-allowed transitions in the energy region around $L_{1v}^{+}\rightarrow L_{2c}^{-}$ (9.45 eV) and $K_{1v}\rightarrow K_{1c}$ (10.27 eV), and to the higher dipole-allowed transitions $X_{1v}^{+}\rightarrow X_{5c}^{-}$ (13.56 eV) and $K_{1v}\rightarrow K_{2c}$ (15.20 eV).

The valence bandwidth has been measured by x-ray photoemission spectroscopy[43,45] (XPS), and we find again a substantial agreement between our theoretical values and the XPS data.

Reflectivity measurements have been performed around the Li^{+} K edge, and a prominent peak at 57.8 eV has been identified as due to a Li^{+} $1s\rightarrow 2p$-allowed exciton at point X. This is confirmed (within the accuracy of the experiments at these energies) by the prominent peak in the Li^{+} K photoelectric yield spectrum[45] occurring at 58.4 eV. In order to estimate the core-conduction energy threshold, we assume that the binding energy of the core exciton is determined by the reduced mass $\mu=0.666m_e$ (see Table IV) and by the electronic contribution to the dielectric constant $\epsilon_0=3.61$. We obtain a binding energy of the core exciton of $E_b^{\text{core}}=0.70$ eV, which is an order of magnitude higher than the binding energy of the valence exciton. An increase in binding energy of core excitons has been observed also in other materials and has been extensively discussed in the literature;[46] this interesting effect seems to be favored whenever the conduction band has minima away from the center of the Brillouin zone because of the intervally mixing among them. For a discussion of a similar effect on impurity states see Ref. 47. Although a rigorous account of the interplay between the central-cell correction and intervalley mixing in determining the binding energy of core excitons is difficult, from the experimental value[45] of the exciton resonance and the theoretical binding energy, we estimate the core-conduction threshold at $\simeq$59.1 eV. From Table III we see again a good agreement with the theoretical value of $X_{1\,\text{core}}^{+}\rightarrow X_{2c}^{-}$ (58.82 eV) in the COHSEX approximation (although this agreement must be taken with some caution because of the already mentioned uncertainty both on the experimental and theoretical side).

Besides the prominent core-exciton peak, other structures were observed at $\simeq$66.0 and $\simeq$70.7 eV in reflectivity measurements,[44] and at $\simeq$63.4 and $\simeq$72 eV in photoelectric Li K yield measurements.[45] The discrepancy of $\simeq$2 eV in the experimental position of these structures is not clear at this stage. We notice here that the position of these structures with respect to the band-to-band threshold seems to be in overall correspondence with the structures of the valence-conduction transitions with respect to the energy gap. A relative shift is expected because of the lack of dispersion of core states and because of the *different selection rules for cationic and anionic s-like bands* (a point which seems to have been overlooked in the literature). According to our results in Table III, the experimental structures in photoelectric Li K yield spectra at $\simeq$63.4 and $\simeq$72 eV seem to be related to the dipole-allowed transitions in the energy region around $K_{1\,\text{core}}\rightarrow K_{1c}$ (63.35 eV) and to the higher dipole-allowed transition $L_{2\,\text{core}}^{-}\rightarrow L_{1c}^{+}$ (70.87 eV) and $L_{2\,\text{core}}^{-}\rightarrow L_{3c}^{+}$ (73.21 eV). Notice that $L_1^{+}+L_3^{+}$ are p-like states for the ion *not* at the origin (i.e., Li^{+} in our work), and the experimental structure in photoelectric yield spectra beginning at $\simeq$72 eV can be assigned to $s\rightarrow p$ cationic transitions (with initial and final energies both shifted by the Madelung term with respect to the free cation). This interpretation is further corroborated by the fact that the transition energy $\Gamma_{1\,\text{core}}^{+}\rightarrow\Gamma_{4c}^{-}$ occurs at 74.73 eV, which is near the experimental ionization limit ($I_p=75.62$ eV) of the free cation. However, further experimental data with better resolution would be desirable in the energy region of core transitions.

TABLE V. Experimental data (in eV) for valence-conduction transition edges, valence bandwidth, and core-conduction edges, and comparison with our QP and HF band-structure calculations.

	$X_{1v}^{+}\rightarrow X_{2c}^{-}$	$L_{1v}^{+}\rightarrow L_{2c}^{-}$	$X_{1v}^{+}\rightarrow X_{5c}^{-}$	$\Delta_v=X_{1v}^{+}-\Gamma_{1v}^{+}$	$X_{1\,\text{core}}^{+}\rightarrow X_{2c}^{-}$	$X_{1\,\text{core}}^{+}\rightarrow X_{5c}^{-}$	$L_{2\,\text{core}}^{-}\rightarrow L_{1c}^{+}$	$L_{2\,\text{core}}^{-}\rightarrow L_{3c}^{+}$
HF	10.80	15.02	19.54	8.20	67.13	75.87	79.51	82.10
COHSEX	5.24	9.45	13.58	7.16	58.82	67.16	70.87	73.11
Expt.					exciton			
	4.99[a]	$\simeq$9.0[b]	$\simeq$13.5[b]	6.3±1.1[c]	58.4[c]	$\simeq$66[b]	above 72[c]	
				6.0±1.5[d]	57.8[b]		above 70.7[b]	

[a] References 39, 40, and 44.
[b] Reference 44.
[c] Reference 45.
[d] Reference 43.

IV. CONCLUSIONS

In this paper we have performed an *ab initio* study of the quasiparticle energy bands in lithium hydride, and we have obtained a satisfactory quantitative understanding of the peculiar physical properties of this compound. Despite its apparent simplicity, the study of the electronic structure must be done with sophisticated techniques. The peculiar shape of the bands, the occurrence of equivalent minima, and the high anisotropy of quasiparticle effective masses add interest to this prototype compound. This work should also stimulate a wider study of quasiparticles in solids, since it is evident that the techniques for solving rigorously HF integro-differential equations can be appropriately transferred to the solution of the integro-differential equations obeyed by the one-particle Green's functions.

ACKNOWLEDGMENTS

We are very grateful to Professor G. Grosso for many invaluable and stimulating discussions. G. Pezzica wishes to thank Professor A. Quattropani for his interest at the École Polytechnique Fédérale de Lausanne, where part of this work has been performed. Financial support from the Italian Ministry of Public Education is also acknowledged.

APPENDIX: ANALYTIC EXPRESSION OF THE SCREENED-EXCHANGE BIELECTRONIC INTEGRALS BETWEEN GAUSSIAN ORBITALS AND PLANE WAVES

In this appendix we give the analytic tools for computing the matrix elements of the self-energy operator in the OPW method. We explicitly discuss here only the expression of the screened-exchange bielectronic integrals because these are by far the most complicated ingredients we need. The other types of integrals are either a particular case of what we are going to discuss explicitly or are trivial. This appendix is presented in a self-contained form; it includes as particular cases, situations already encountered in previous papers.[9,37] Without loss of generality, we suppose that the GTO's of interest are of $1s$ type; higher angular momenta can be easily handed by applying differentiation techniques to the results of the present Appendix.

The most general screened-exchange bielectronic integral we need in our calculation on LiH involves two plane waves and two $1s$ GTO's, centered on different sites, i.e.,

$$J_s(\mathbf{k}_1,\alpha_1,\boldsymbol{\delta}_1;\lambda;\mathbf{k}_2,\alpha_2,\boldsymbol{\delta}_2)=\int e^{-i\mathbf{k}_1\cdot\mathbf{r}_1}e^{-\alpha_1(\mathbf{r}_1-\boldsymbol{\delta}_1)^2}\frac{e^{-\lambda r_{12}}}{r_{12}}e^{i\mathbf{k}_2\cdot\mathbf{r}_2}e^{-\alpha_2(\mathbf{r}_2-\boldsymbol{\delta}_2)^2}d\mathbf{r}_1d\mathbf{r}_2\,, \tag{A1}$$

where $r_{12}=|\mathbf{r}_1-\mathbf{r}_2|$. An analytic expression for J_s can be obtained in terms of the error function of complex argument.

First we decouple the variables $\mathbf{r}_1$ and $\mathbf{r}_2$ by means of the identity

$$\frac{e^{-\lambda r_{12}}}{r_{12}}=\frac{1}{2\pi^2}\int\frac{e^{i\mathbf{q}\cdot(\mathbf{r}_1-\mathbf{r}_2)}}{q^2+\lambda^2}d\mathbf{q}\,.$$

Then we exploit the well-known relation for the Fourier transform of a Gaussian function

$$\int e^{i\mathbf{k}\cdot\mathbf{r}}e^{-\alpha(\mathbf{r}-\boldsymbol{\delta})^2}d\mathbf{r}=\left[\frac{\pi}{\alpha}\right]^{3/2}e^{i\mathbf{k}\cdot\boldsymbol{\delta}}e^{-k^2/4\alpha}\,. \tag{A2}$$

With some trivial algebra we obtain

$$J_s=\frac{\pi}{2(\alpha_1\alpha_2)^{3/2}}e^{-i(\mathbf{k}_1\cdot\boldsymbol{\delta}_1-\mathbf{k}_2\cdot\boldsymbol{\delta}_2)}e^{-(k_1^2/4\alpha_1)-(k_2^2/4\alpha_2)}$$
$$\times\int e^{i\mathbf{q}\cdot\boldsymbol{\chi}_{12}}\frac{e^{-q^2/4\alpha_{12}}}{q^2+\lambda^2}d\mathbf{q}\,, \tag{A3}$$

where the reduced exponent α_{12} and the vector $\boldsymbol{\chi}_{12}$ are defined as

$$\alpha_{12}=\frac{\alpha_1\alpha_2}{\alpha_1+\alpha_2}\,,\quad \boldsymbol{\chi}_{12}=\boldsymbol{\delta}_1-\boldsymbol{\delta}_2-i\left[\frac{\mathbf{k}_1}{2\alpha_1}+\frac{\mathbf{k}_2}{2\alpha_2}\right].$$

The problem of evaluating J_s has been transformed into the problem of finding an analytic solution for the integral

$$I=\int e^{i\mathbf{q}\cdot\boldsymbol{\chi}}\frac{e^{-q^2/4\alpha}}{q^2+\lambda^2}d\mathbf{q}\,, \tag{A4}$$

where $\boldsymbol{\chi}$ is a complex vector (the subscript to $\boldsymbol{\chi}$ and α have been suppressed, being inessential here).

We use the identity

$$\frac{1}{q^2+\lambda^2}=\int_0^\infty e^{-\beta(q^2+\lambda^2)}d\beta\,,$$

next we analytically extend to the case of the complex $\mathbf{k}$ vector the result (A2) valid in real field. We obtain

$$I=\int_0^\infty\left[\frac{\pi}{\beta+(1/4\alpha)}\right]^{3/2}e^{-\beta\lambda^2}e^{-[\chi^2/4(\beta+1/4\alpha)]}d\beta$$
$$=e^{\lambda^2/4\alpha}\int_{1/4\alpha}^\infty\left[\frac{\pi}{\beta}\right]^{3/2}e^{-\beta\lambda^2}e^{-\chi^2/4\beta}d\beta\,,$$

where $\chi^2=\chi_x^2+\chi_y^2+\chi_z^2$. Performing the change of variable

$$t^2=\frac{\chi^2}{4\beta}\,,\quad d\beta=-\frac{\chi^2}{2t^3}dt$$

the expression for I becomes

$$I=\frac{4\pi^{3/2}}{\chi}e^{\lambda^2/4\alpha}\int_0^{\chi\sqrt{\alpha}}e^{-t^2-(\chi^2\lambda^2/4t^2)}dt\ , \tag{A5}$$

where for χ one means

$$\chi=(\boldsymbol{\chi}\cdot\boldsymbol{\chi})^{1/2}\ . \tag{A6}$$

It is useful to introduce at this stage the complex error function[48] erf(z):

$$\mathrm{erf}(z)=\frac{2}{\sqrt{\pi}}\int_0^z e^{-t^2}dt\ ,\quad z\in\mathbb{C}\ .$$

Using the following indefinite integral,

$$\int e^{-a^2x^2-(b^2/x^2)}dx = \frac{\sqrt{\pi}}{4a}\left[e^{2ab}\,\mathrm{erf}\left[ax+\frac{b}{x}\right]+e^{-2ab}\,\mathrm{erf}\left[ax-\frac{b}{x}\right]\right] + \text{const}\ ,$$

and with some algebra, we arrive at the result

$$I=\frac{\pi^2}{\chi}e^{\lambda^2/4\alpha}\left\{e^{\lambda\chi}\left[\mathrm{erf}\left[\chi\sqrt{\alpha}+\frac{\lambda}{2\sqrt{\alpha}}\right]-1\right] +e^{-\lambda\chi}\left[\mathrm{erf}\left[\chi\sqrt{\alpha}-\frac{\lambda}{2\sqrt{\alpha}}\right]+1\right]\right\}. \tag{A7}$$

It is easily verified that Eq. (A7) does not depend on the sign of χ; in fact, if we change $\chi\rightarrow-\chi$, the integral I is invariant because of the standard odd property of the complex error function $\mathrm{erf}(-z)=-\mathrm{erf}(z)$. The final result for J_s is quite simple:

$$J_s(\mathbf{k}_1,\alpha_1,\boldsymbol{\delta}_1;\lambda;\mathbf{k}_2,\alpha_2,\boldsymbol{\delta}_2)=\frac{\pi^3}{2(\alpha_1\alpha_2)^{3/2}}e^{-i(\mathbf{k}_1\cdot\boldsymbol{\delta}_1-\mathbf{k}_2\cdot\boldsymbol{\delta}_2)}e^{-(k_1^2/4\alpha_1)-(k_2^2/4\alpha_2)}\frac{e^{\lambda^2/4\alpha_{12}}}{\chi_{12}} \times\left\{e^{\lambda\chi_{12}}\left[\mathrm{erf}\left[\chi_{12}\sqrt{\alpha_{12}}+\frac{\lambda}{2\sqrt{\alpha_{12}}}\right]-1\right]+e^{-\lambda\chi_{12}}\left[\mathrm{erf}\left[\chi_{12}\sqrt{\alpha_{12}}-\frac{\lambda}{2\sqrt{\alpha_{12}}}\right]+1\right]\right\}. \tag{A8}$$

An equivalent expression, useful for the computational work, can be obtained using the relation

$$\mathrm{erf}(z)=1-e^{-z^2}w(iz)\ ,$$

where the complex function $w(z)$ is defined[48] as

$$w(z)=e^{-z^2}\left[1+\frac{2i}{\sqrt{\pi}}\int_0^z e^{t^2}dt\right].$$

Equation (A8) can be written as

$$J_s=\frac{\pi^3}{2(\alpha_1\alpha_2)^{3/2}}e^{-i(\mathbf{k}_1\cdot\boldsymbol{\delta}_1-\mathbf{k}_2\cdot\boldsymbol{\delta}_2)}e^{-(k_1^2/4\alpha_1)-(k_2^2/4\alpha_2)}\frac{e^{-\alpha_{12}\chi_{12}^2}}{\chi_{12}} \times\left[w\left[i\left[\frac{\lambda}{2\sqrt{\alpha_{12}}}-\sqrt{\alpha_{12}}\chi_{12}\right]\right]-w\left[i\left[\frac{\lambda}{2\sqrt{\alpha_{12}}}+\sqrt{\alpha_{12}}\chi_{12}\right]\right]\right]. \tag{A9}$$

With the help of a standard computer routine[49,50] for the function $w(z)$ the screened-exchange integrals can be easily evaluated.

*Present address: Istituto di Fisica Teorica, Università di Trieste, Strada Costiera 11, 3401 Miramare, Grignano, Italy and Gruppo Nazionale di Struttura della Materia del Consiglio Nazionale delle Ricerche, Piazza Torricelli 2, 56100 Pisa, Italy.

[1]See, for example, N. E. Brener and J. L. Fry, Phys. Rev. B **17**, 506 (1978); **19**, 1720 (1979), and references quoted therein.

[2]L. Hedin, Phys. Rev. **139**, A796 (1965); Ark. Fys. **30**, 231 (1965).

[3]L. Hedin and S. Lundqvist, in *Solid State Physics,* edited by F. Seitz, D. Turnbull, and H. Ehrenreich (Academic, New York, 1969), Vol. 23, p. 1, and references quoted therein.

[4]W. Brinkman and B. Goodman, Phys. Rev. **149**, 597 (1966).

[5]N. O. Lipari and W. B. Fowler, Phys. Rev. B **2**, 3354 (1970).

[6]N. E. Brener, Phys. Rev. B **11**, 929, 1600 (1975).

[7]P. Hohenberg and W. Kohn, Phys. Rev. **136**, B864 (1964); W. Kohn and L. J. Sham, *ibid.* **140**, A1133 (1965). See also, for example, J. P. Perdew and A. Zunger, Phys. Rev. B **23**, 5048 (1981); S. Baroni and E. Tuncel, J. Chem. Phys. **79**, 6140 (1983). For an up-to-date review on density-functional theories, see W. Kohn and P. Vashista, in *Theory of the Inhomogeneous Electron Gas,* edited by N. H. March and S. Lundqvist (Plenum, New York, 1983).

[8]See, for example, G. Strinati, H. J. Mattausch, and W. Hanke,

Phys. Rev. B **25**, 2867 (1982); S. Horsch, P. Horsch, and P. Fulde, *ibid.* **28**, 5977 (1983); **29**, 1870 (1984); A. W. Overhauser, in *Electron Correlations in Solids, Molecules and Atoms,* edited by J. T. Devreese and F. Brosen (Plenum, New York, 1983), p. 41; H. Yasuhara, in *Electron Correlations in Solids, Molecules and Atoms,* p. 411.

[9]S. Baroni, G. Grosso, and G. Pastori Parravicini, Phys. Rev. B **29**, 2891 (1984).

[10]S. F. Boys, Proc. R. Soc. London **A200**, 542 (1950). For a review see, for example, I. Shavitt, in *Methods in Computational Physics,* edited by B. Alder, S. Ferbach, and M. Rotenberg (Academic, New York, 1963), and references quoted therein.

[11]C. Herring, Phys. Rev. **57**, 1169 (1940). See also T. O. Woodruff, *Solid State Physics,* edited by F. Seitz and D. Turnbull (Academic, New York, 1957), Vol. 4, p. 367. The generalization of the orthogonalized-plane-wave method to the many-body problem was first considered by F. Bassani, J. Robinson, B. Goodman, and J. R. Schrieffer, Phys. Rev. **127**, 1969 (1962).

[12]E. A. Hylleraas, Z. Phys. **63**, 771 (1930).

[13]R. Dovesi, C. Ermondi, E. Ferrero, C. Pisani, and C. Roetti, Phys. Rev. B **29**, 3591 (1984).

[14]D. H. Ewing and F. Seitz, Phys. Rev. **50**, 760 (1936).

[15]A. B. Kunz and D. J. Mickish, J. Phys. C **6**, L83 (1973); Phys. Rev. B **11**, 1700 (1975).

[16]A. N. Ermoshkin and R. A. Evarestov, Phys. Status Solidi B **66**, 687 (1974).

[17]F. Perrot, Phys. Status Solidi B **77**, 517 (1976).

[18]N. I. Kulikov, Fiz. Tverd. Tela (Leningrad) **20**, 2027 (1978) [Sov. Phys.—Solid State **20**, 1170 (1978)].

[19]G. Grosso and G. Pastori Parravicini, Phys. Rev. B **20**, 2366 (1979).

[20]J. L. Anderson, J. Nasise, K. Philipson, and F. E. Pretzel, J. Phys. Chem. Solids **31**, 613 (1970); A. R. Ruffa, Phys. Rev. B **27**, 1321 (1983).

[21]R. P. Hurst, Phys. Rev. **114**, 746 (1959).

[22]K. O-ohata, H. Taketa, and S. Huzinaga, J. Phys. Soc. Jpn. **21**, 2306 (1966); **21**, 2313 (1966); W. J. Hehre, R. F. Stewart, and J. A. Pople, J. Chem. Phys. **51**, 2657 (1969).

[23]P. O. Löwdin, Phys. Rev. **97**, 1474 (1955); **97**, 1490 (1955); **97**, 1509 (1955); Adv. Phys. **5**, 1 (1956).

[24]K. F. Berggren and F. Martino, Phys. Rev. B **3**, 1509 (1971).

[25]See, for example, S. Ameri, G. Grosso, and G. Pastori Parravicini, Phys. Rev. B **23**, 4242 (1981), and references quoted therein.

[26]E. Tosatti and G. Pastori Parravicini, J. Phys. Chem. Solids **32**, 623 (1971); Z. H. Levine and S. G. Louie, Phys. Rev. B **25**, 6310 (1982), and references quoted therein.

[27]E. Staritzky and D. J. Walker, Anal. Chem. **28**, 1055 (1956). See also F. E. Pretzel, G. N. Rupert, C. L. Mader, E. K. Storms, G. V. Gritton, and C. C. Rushing, J. Phys. Chem. Solids **16**, 10 (1960); M. H. Brodsky and E. Burstein, J. Phys. Chem. Solids **28**, 1655 (1967).

[28]See, for example, R. Resta, Phys. Rev. B **16**, 2717 (1977).

[29]C. E. Moore, *Atomic Energy Levels,* U.S. National Bureau of Standards Circular No. 467 (U.S. GPO, Washington D.C., 1958).

[30]M. P. Tosi, *Solid State Physics,* edited by F. Seitz and D. Turnbull (Academic, New York, 1964), Vol. 16, p. 1.

[31]G. F. Koster, J. O. Dimmock, R. C. Wheeler, and H. Statz, *Properties of the Thirty-two Point Groups* (MIT, Cambridge, Mass., 1963).

[32]T. Paakkari, V. Halonen, and O. Aikala, Phys. Rev. B **13**, 4602 (1976).

[33]F. Bassani and E. S. Giuliano, Nuovo Cimento B **8**, 193 (1972), and references quoted therein.

[34]F. Bassani and G. Pastori Parravicini, *Electronic States and Optical Transitions in Solids* (Pergamon, Oxford, 1975).

[35]A. B. Kunz, Phys. Rev. B **26**, 2056 (1982).

[36]G. Pastori Parravicini, I. Villa, and M. Vittori, Phys. Status Solidi B **67**, 345 (1975); C. Friedli and N. W. Ashcroft, Phys. Rev. B **16**, 662 (1977).

[37]P. Giannozzi and S. Baroni, Phys. Rev. B **30**, 7187 (1984).

[38]V. G. Plekhanov, V. A. Pustovarov, A. A. O'Connell-Bronin, T. A. Betenekova, and S. O. Cholakh, Fiz. Tverd. Tela (Leningrad) **18**, 2438 (1976) [Sov. Phys.—Solid State **18**, 1422 (1976)].

[39]G. S. Zavt, K. A. Kalder, I. L. Kuusmann, Ch. B. Lushchik, V. G. Plekhanov, S. O. Cholakh, and R. A. Evarestov, Fiz. Tverd. Tela (Leningrad) **18**, 2724 (1976) [Sov. Phys.—Solid State **18**, 1588 (1976)].

[40]V. G. Plekhanov, A. A. O'Connell-Bronin, and T. A. Betenekova, Fiz. Tverd. Tela (Leningrad) **19**, 3297 (1977) [Sov. Phys.—Solid State **19**, 1926 (1977)].

[41]V. G. Plekhanov, G. S. Zavt, T. A. Betenekova, A. A. O'Connell-Bronin, and S. O. Cholakh, Solid State Commun. **25**, 159 (1978).

[42]V. G. Plekhanov and A. A. O'Connell-Bronin, Fiz. Tverd. Tela (Leningrad) **20**, 2078 (1978) [Sov. Phys.—Solid State **20**, 1200 (1978)].

[43]T. A. Betenekova, S. O. Cholakh, I. M. Shabanova, V. A. Trapeznikov, F. F. Gavrilov, and B. V. Shul'gin, Fiz. Tverd. Tela (Leningrad) **20**, 2470 (1978) [Sov. Phys.—Solid State **20**, 1426 (1978)].

[44]T. Miki, M. Ikeya, Y. Kondo, and H. Kanzaki (unpublished); Solid State Commun. **39**, 647 (1981).

[45]K. Ichikawa, N. Suzuki, and K. Tsutsumi, J. Phys. Soc. Jpn. **50**, 3650 (1981).

[46]A. Quattropani, F. Bassani, G. Margaritondo, and G. Tinivella, Nuovo Cimento B **51**, 335 (1979); G. Iadonisi and F. Bassani, Nuovo Cimento **3**, 408 (1984).

[47]L. Resca, Phys. Rev. B **29**, 866 (1984), and references quoted therein.

[48]*Handbook of Mathematical Functions,* edited by M. Abramowitz and I. A. Stegun (Dover, New York, 1972).

[49]W. Gautschi, SIAM (Soc. Ind. Appl. Math.) J. Numer Anal. **7**, 187 (1970).

[50]W. Gautschi, Commun. ACM **12**, 635 (1969); see algorithm 363. A Fortran translation of the above Algol algorithm is filed in the European Organization for Nuclear Research (CERN) program library; this translation has been rewritten for our purposes with double precision.